

JunB transcription factor maintains skeletal muscle mass and promotes hypertrophy

Anna Raffaello,^{1,5} Giulia Milan,^{3,4} Eva Masiero,^{3,4} Silvia Carnio,^{3,4} Donghoon Lee,⁵ Gerolamo Lanfranchi,¹ Alfred Lewis Goldberg,⁵ and Marco Sandri^{2,3,4}

¹Department of Biology, Innovative Biotechnologies Interdepartmental Research Center and ²Department of Biomedical Sciences, University of Padova, 35122 Padova, Italy

³Venetian Institute of Molecular Medicine, 35129 Padova, Italy

⁴Dulbecco Telethon Institute, 35129 Padova, Italy

⁵Department of Cell Biology, Harvard Medical School, Boston, MA 02115

The size of skeletal muscle cells is precisely regulated by intracellular signaling networks that determine the balance between overall rates of protein synthesis and degradation. Myofiber growth and protein synthesis are stimulated by the IGF-1/Akt/mammalian target of rapamycin (mTOR) pathway. In this study, we show that the transcription factor JunB is also a major determinant of whether adult muscles grow or atrophy. We found that in atrophying myotubes, JunB is excluded from the nucleus and that decreasing JunB expression by RNA interference in adult muscles causes atrophy.

Furthermore, JunB overexpression induces hypertrophy without affecting satellite cell proliferation and stimulated protein synthesis independently of the Akt/mTOR pathway. When JunB is transfected into denervated muscles, fiber atrophy is prevented. JunB blocks FoxO3 binding to atrogin-1 and MuRF-1 promoters and thus reduces protein breakdown. Therefore, JunB is important not only in dividing populations but also in adult muscle, where it is required for the maintenance of muscle size and can induce rapid hypertrophy and block atrophy.

Introduction

Skeletal muscles comprise 40–50% of total body mass and constitute the major protein reservoir of the organism. When muscle mass decreases in fasting and in many systemic diseases, amino acids from muscle proteins are mobilized to provide substrates for hepatic gluconeogenesis and for the synthesis of critical proteins. The resulting loss of muscle mass in these catabolic states and upon denervation or disuse involves a common transcriptional program (Sandri et al., 2004, 2006; Stitt et al., 2004; Zhao et al., 2007), resulting in a general acceleration of proteolysis and a decrease in protein synthesis in most catabolic states (Furuno et al., 1990; Medina et al., 1995; Wing et al., 1995; Mitch and Goldberg, 1996; Jagoe and Goldberg, 2001; Glass, 2005; Kandarian and Jackman, 2006). We have identified a set of ~100 atrophy-related genes or “atrogenes” whose expression increases

and decreases similarly in various types of muscle atrophy (Lecker et al., 2004; Sackey et al., 2007). Among the genes induced most dramatically during atrophy are two muscle-specific ubiquitin ligases, *atrogin-1/MAFbx* (muscle atrophy F-box) and *MuRF-1* (muscle RING finger-1; Lecker et al., 2004; Sackey et al., 2007), whose induction is essential for rapid atrophy (Bodine et al., 2001a; Gomes et al., 2001; Jagoe et al., 2002). Activation of the FoxO transcription factors has been shown to be crucial in the development of muscle wasting and for the induction of *atrogin-1* and *MuRF-1* (Sandri et al., 2004; Stitt et al., 2004). Moreover, activation of FoxO3 by itself is sufficient to cause dramatic atrophy (Sandri et al., 2004).

In growing muscles, FoxOs are maintained in an inactive state by the IGF-1/phosphoinositide 3-kinase (PI3K)/Akt signaling cascade (Sandri et al., 2004). This pathway plays a key role in the regulation of muscle mass (Bodine et al., 2001b;

Correspondence to: Marco Sandri: marco.sandri@unipd.it; Gerolamo Lanfranchi: gerolamo.lanfranchi@unipd.it; or Alfred L. Goldberg: alfred_goldberg@hms.harvard.edu

Abbreviations used in this paper: AP-1, activator protein-1; ca-FoxO3, constitutively active FoxO3; ChIP, chromatin immunoprecipitation; mTOR, mammalian target of rapamycin; MyHC-2B, myosin heavy chain type 2B; PI3K, phosphoinositide 3-kinase; shRNA, small hairpin RNA; Smad, small mother against decapentaplegic; TA, tibialis anterior.

© 2010 Raffaello et al. This article is distributed under the terms of an Attribution–Noncommercial–Share Alike–No Mirror Sites license for the first six months after the publication date [see <http://www.rupress.org/terms>]. After six months it is available under a Creative Commons License (Attribution–Noncommercial–Share Alike 3.0 Unported license, as described at <http://creativecommons.org/licenses/by-nc-sa/3.0/>).

Rommel et al., 2001) and promotes fiber hypertrophy by stimulating overall protein synthesis and suppressing proteolysis. In skeletal muscle, activation of Akt by IGF-1 stimulates protein translation through induction of mammalian target of rapamycin (mTOR), which activates p70S6K and inactivates the inhibitor of translational initiation 4EBP1 (Bodine et al., 2001b; Rommel et al., 2001), and GSK-3 β , which stimulates the initiation factor eIF2B. In addition, Akt suppresses muscle protein breakdown mainly by phosphorylating FoxO3, which leads to its inactivation through sequestration in the cytosol (Sandri et al., 2004; Stitt et al., 2004). In contrast, during atrophy, the activity of the IGF-1/PI3K/Akt pathway decreases, leading to the activation of FoxO3, which leads to a stimulation of protein breakdown not only by the ubiquitin–proteasome pathway (Sandri et al., 2004; Stitt et al., 2004) but also by the autophagic/lysosomal system (Mammucari et al., 2007; Zhao et al., 2007).

Although many transcription factors have been implicated in the differentiation of muscle and in muscle atrophy, none has been shown to promote growth of adult muscle. Here, we demonstrate that the transcription factor JunB is sufficient to promote muscle growth independently of changes in the Akt pathway. JunB attracted our attention because we had found that its mRNA was markedly down-regulated in muscle during various types of atrophy, including denervation, disuse, fasting, diabetes, sepsis, acidosis, and cancer cachexia (Lecker et al., 2004; Sackey et al., 2004). This transcription factor belongs to the activator protein-1 (AP-1) family, which includes both the Jun and also Fos families (Angel et al., 1987, 1988; Curran and Franz, 1988; Halazonetis et al., 1988; Hirai and Yaniv, 1989), and we had found that during starvation in myotubes, the DNA binding activity of nuclear extracts to the AP-1 binding sites decreases (Sandri et al., 2004). *JunB* and *Fos* belong to a class of immediate early genes that are rapidly activated, usually transiently, in response to cytokines, growth factors, stress signals, infection, or oncogenic stimuli (Sng et al., 2004). Every cell type contains a complex mixture of AP-1 dimers with subtly different functions (Wagner, 2001), which respond to various physiological and pathological stimuli.

However, JunB function has been investigated primarily in dividing cell populations, and its role in skeletal muscle or other postmitotic tissues has been barely studied. Treatment of cardiac myocytes with insulin was found to stimulate the binding of the AP-1 transcription factor to its specific consensus sequence (Markou et al., 2008). This observation, together with the decrease of *JunB* expression during atrophy (Lecker et al., 2004; Sackey et al., 2007), suggested that an AP-1 factor might play an important role in the maintenance of muscle mass and that the decrease in its transcriptional activity might contribute to the loss of muscle mass in atrophic conditions.

Results

JunB is required for maintenance of muscle mass

We previously found that the DNA-binding activity of nuclear extracts to the AP-1 binding sites decreases during starvation in myotubes (Sandri et al., 2004). To learn whether conditions that

trigger atrophy might decrease JunB levels in the nucleus, we measured the amount of this protein in nuclear and cytosolic fractions of differentiated C2C12 myotubes treated with the glucocorticoid dexamethasone for 24 h or after removal of growth medium for 5 h (Fig. 1 A). These treatments induce protein loss and many of the biochemical features of muscle atrophy in adult animals (Bodine et al., 2001b; Gomes et al., 2001; Sackey et al., 2004; Sandri et al., 2004; Stitt et al., 2004). After both treatments, the levels of JunB protein were dramatically reduced in the nucleus (Fig. 1 A), whereas no change was apparent in the cytosolic fraction (Fig. 1 A).

To determine the physiological consequences of this fall in nuclear JunB, we decreased the JunB content of adult mouse muscles using JunB RNAi, and we studied the effects of its inhibition on muscle mass. A vector expressing small hairpin RNAs (shRNAs) against JunB, which specifically blocked JunB expression in murine embryonic fibroblast cells (Fig. S3, A and B), was electroporated into tibialis anterior (TA) muscles. This technique allows high transfection efficiency of myofibers without causing significant damage or inflammation and has been very useful in clarifying regulatory mechanisms in muscle (Sandri et al., 2004, 2006; Mammucari et al., 2007; Sartori et al., 2009; Romanello et al., 2010). Moreover, with our electroporation protocol, only adult myofibers are transfected and not interstitial cells or satellite cells, the muscle stem cells (Figs. 1 B and S1, A–D). To knock down target proteins in vivo for days or weeks, we used bicistronic vectors that simultaneously encode for shRNAs and GFP. Therefore, detection of GFP fluorescence allows us to monitor the efficiency of transfection and the changes in size of myofibers containing shRNAs. Thus, we transfected adult TA muscles with vectors producing shRNAs specific for JunB or unrelated oligos (scramble). Dystrophin staining confirmed that we successfully transfected adult myofibers and not interstitial cells (Fig. 1 B). JunB levels dramatically fell in muscles that were transfected with specific oligos against JunB (Fig. 1 C). When expressed in vivo for 12 d, the shRNA caused a 20% reduction in the mean cross-sectional area (Fig. 1, D and E) below levels in control fibers electroporated with scramble shRNA. To examine the effect of a more prolonged reduction in JunB content, we transfected TA muscles with JunB RNAi and scramble as a control and collected the muscles 1 mo later. JunB knockdown for 1 mo resulted in a 25% reduction in myofiber size (Fig. 1 F). Thus, in normal adult muscle, JunB is required for the maintenance of muscle mass, and its down-regulation or nuclear exclusion causes a prolonged loss of muscle mass.

JunB stimulates protein synthesis and hypertrophy of adult muscle fibers independently of Akt and mTOR

These RNAi-mediated decreases in muscle mass (Fig. 1, D–F) prompted us to investigate whether, conversely, JunB overexpression can promote muscle growth. To learn whether JunB expression induces hypertrophy, we electroporated a plasmid encoding JunB into the TA muscles of adult mice. Dystrophin and Hoechst staining confirmed that JunB was expressed only in adult fibers and was correctly localized only in the myonuclei (Fig. 2 A). JunB overexpression for 9 d caused dramatic hypertrophy of the

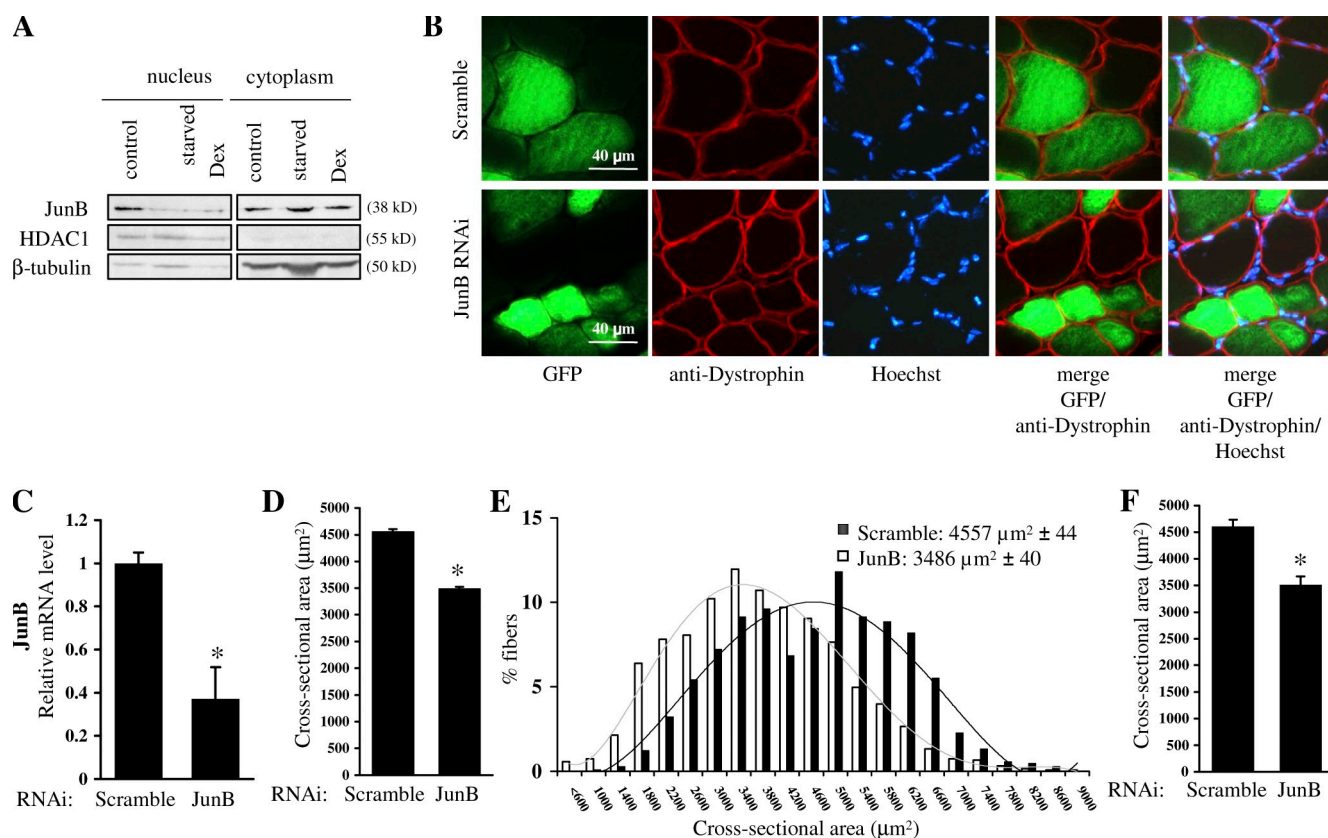


Figure 1. JunB is decreased in the nuclei of atrophying myotubes, and its down-regulation in adult muscles induces muscle atrophy. (A) JunB protein levels in C2C12 myotubes either untreated, starved, or by treatment with dexamethasone. Nuclear and cytosolic fractions were immunoblotted for JunB, nuclear (HDAC1), and cytoplasmic (β -tubulin) proteins. (B–F) The down-regulation of JunB expression induces atrophy. Adult skeletal muscles were transfected with vectors expressing shRNA against JunB or scramble for 12 d. (B) Cryosections were stained for dystrophin to identify plasma membrane (sarcolemma) of myofibers and counterstained with Hoechst. Images were merged to demonstrate that the GFP signal lay under the sarcolemma and not in interstitial cells. (C) JunB mRNA levels measured after transfection of TA muscles with scramble oligos or specific shRNA against JunB. $n = 4$; means \pm SD. (D) Mean cross-sectional areas of 500 fibers expressing the control siRNA (scramble) and fibers expressing shRNA against JunB for 12 d \pm SEM. $n = 4$. (C and D) *, $P < 0.005$. (E) Frequency histograms of the cross-sectional area of fibers with JunB knockdown (open bars) compared with fibers expressing control scramble oligos (shaded bars). $n = 4$. The numeric data are expressed as the mean fiber sizes \pm SEM. (F) The bar diagram represents the mean cross-sectional areas of fibers expressing the control siRNA (scramble) and fibers expressing shRNA against JunB for 1 mo. The experiment was performed as in D. *, $P < 0.01$.

transfected fibers (Fig. 2, B and C). The mean cross-sectional area of these fibers was $\sim 40\%$ greater than that of neighboring nontransfected fibers within the same muscle or fibers transfected with mock plasmid (Fig. 2, B and C). In contrast, transfection of another AP-1 family member, c-Jun, did not affect myofiber size (Fig. 2 B), indicating that the capacity to increase muscle mass is a specific action of JunB.

Hypertrophy of a cell occurs when its overall rate of protein synthesis exceeds the overall rate of protein degradation. To test whether JunB induced growth by increasing protein synthesis, we measured rates of synthesis in myotubes infected with adenoviruses expressing either JunB or GFP (mock plasmid; Fig. 3 A). Within 12 h of infection, JunB enhanced [^3H]tyrosine incorporation into protein by 50%, and this effect was then maintained for the course of the experiment. These findings make it likely that the rapid hypertrophy induced by JunB in adult fibers is a result of enhanced protein synthesis. To confirm the importance of increased synthesis in vivo (Fig. 2, B and C), TA muscles were electroporated with the JunB expression vector, and, 4 d later, animals were treated with cycloheximide as described in Fan et al. (2010) to inhibit protein synthesis. Cycloheximide significantly decreased the growth of the

transfected fibers (Fig. S2 B). Together, these findings, along with the lack of effect of JunB on basal protein degradation (see the next paragraph), indicate that JunB induces hypertrophy of normal muscles by stimulating protein synthesis.

Surprisingly, this stimulation of protein synthesis in the myotubes occurred independently of any clear activation (i.e., phosphorylation) of components of the PI3K/Akt/mTOR pathway (Fig. 3 B), in sharp contrast to the stimulation of synthesis by IGF-1 or insulin (Bodine et al., 2001b; Rommel et al., 2001). Specifically, we did not observe increases in either the total level or the phosphorylated forms of the key components of this pathway (e.g., Akt or S6K) that are generally believed to be crucial for muscle hypertrophy (Bodine et al., 2001b; Rommel et al., 2001). On the contrary, JunB overexpression actually decreased the levels of phosphorylated Akt, S6K, and 4EBP1 without affecting the amount of the TORC1 proteins mTOR and raptor (Fig. 3 B). Furthermore, when a similar analysis was performed on components of the PI3K/Akt pathway in TA mouse muscles during hypertrophy induced by JunB electroporation for 9 d, there was no evidence of activation of this pathway, as was found in myotubes (Fig. S3 C).

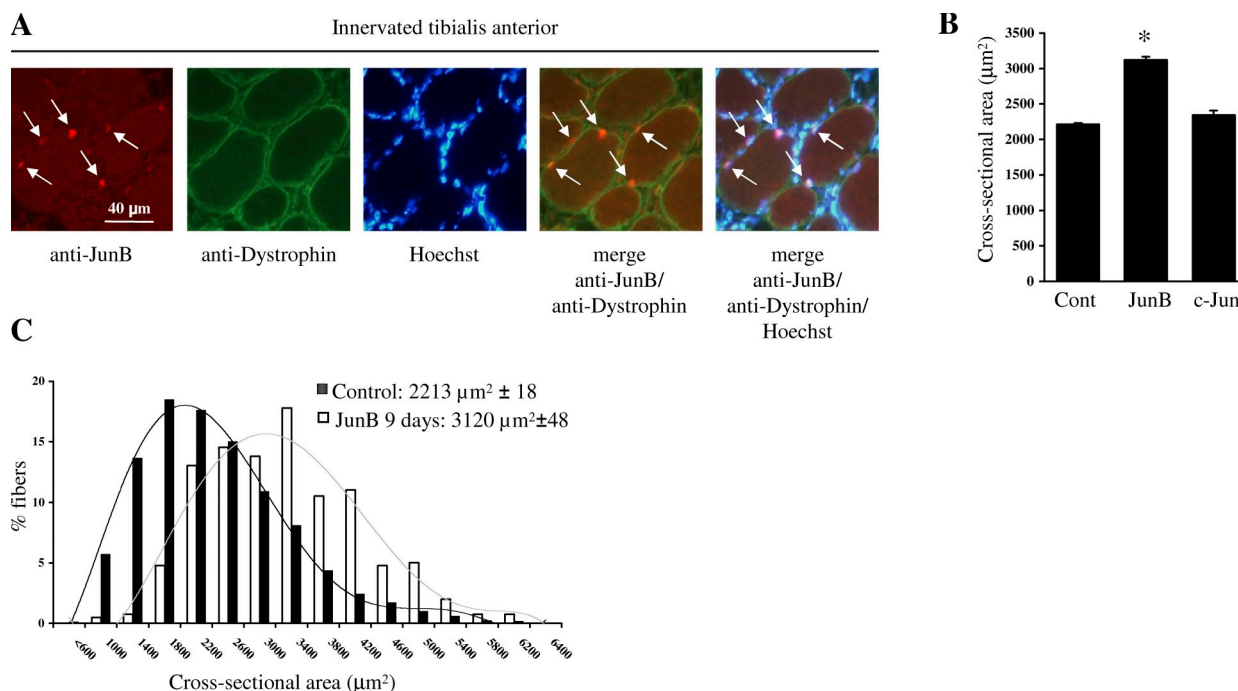


Figure 2. JunB stimulates the growth of fibers in TA muscles. TA muscles of adult mice were electroporated with JunB and were analyzed 9 d later. (A) Localization of JunB and dystrophin. Images were merged to demonstrate that the JunB-positive nuclei lay under the sarcolemma. The arrows indicate the myonuclei overexpressing JunB. (B) JunB, but not c-Jun, causes myotube hypertrophy. Mean cross-sectional area of transfected fibers overexpressing either JunB or c-Jun for 9 d compared with the area of the surrounding untransfected myofibers (control). For each condition, at least 500 fibers were counted, $n = 4$. Values are means \pm SEM. *, $P < 0.001$. (C) Frequency histograms showing the distribution of cross-sectional areas of ~ 500 fibers expressing JunB for 9 d (open bars) and an equal number of surrounding nontransfected fibers (control fibers; shaded bars). The numeric data are expressed as the mean fiber areas \pm SEM, $n = 4$.

Because this apparent enhancement of synthesis without activation of mTOR was surprising, we further tested these conclusions by blocking mTORC1 activity with rapamycin treatment in myotubes overexpressing JunB or GFP (mock plasmid; Fig. 3 C). Rapamycin reduced [^3H]tyrosine incorporation into protein in control myotubes by 29%, but JunB overexpression maintained protein synthesis at control levels despite the presence of rapamycin (Fig. 3 C). To our knowledge, these findings represent the first example of a stimulation of overall protein synthesis and hypertrophy of muscle that is independent of Akt or mTOR.

To confirm this conclusion *in vivo*, we transfected JunB into adult muscle of transgenic mice expressing tamoxifen-inducible Akt specifically in skeletal muscle (Mammucari et al., 2007). As expected, activation of Akt expression in muscle induced hypertrophy, but the overexpression of JunB further increased the mean myofiber cross-sectional area by $\sim 50\%$ (Fig. 3 D). Together, these findings show that the stimulation of synthesis by JunB and Akt is independent and additive.

In addition, we tested whether JunB-mediated hypertrophy involves the activation and fusion of satellite cells, the muscle stem cells. To test this possibility, we treated mice with BrdU after transfection. 9 d later, we monitored for incorporation of BrdU-positive nuclei into fibers expressing JunB. However, we never detected BrdU in myonuclei of transfected fibers (Fig. S2 A, left). In control experiments, we could confirm efficient incorporation of BrdU into myonuclei in damaged muscles undergoing regeneration (Fig. S2 A, right). Thus, JunB-mediated hypertrophy does not require activation and recruitment of satellite cells.

Because contractile proteins comprise $>40\%$ of total muscle proteins, we tested whether JunB, while stimulating muscle hypertrophy, affects myosin gene expression. We cotransfected JunB and a promoter reporter construct for fast (myosin heavy chain type 2B [MyHC-2B]) myosin into the glycolytic fast TA muscle. JunB greatly enhanced transcription of the MyHC-2B promoter (Fig. 3 E). This finding is noteworthy because MyHC-2B is the most abundant myosin in TA muscles and is induced during fiber hypertrophy. Furthermore, we observed a similar increase in MyHC-2B mRNA in myotubes overexpressing JunB by adenovirus infection (Fig. 3 F). In addition, chromatin immunoprecipitation (ChIP) analysis confirmed the binding of JunB to the MyHC-2B promoter (Fig. 3 G). Thus, JunB promotes hypertrophy by enhancing overall protein synthesis and by activating myosin expression.

JunB blocks muscle atrophy and inhibits atrogen-1 and MuRF-1 induction

Because of JunB's ability to enhance protein synthesis and to promote growth of adult muscles *in vivo*, we tested whether JunB could inhibit denervation atrophy of mouse muscles. The sciatic nerve in adult mice was cut to induce rapid atrophy of the TA muscle, and, at the same time, a JunB expression vector was transfected into the muscle. 9 d later, the denervated, untransfected fibers decreased in mean cross-sectional area by 30% compared with fibers in the controlateral innervated muscle (Fig. 4, B and C). However, overexpression of JunB in the denervated fibers (Fig. 4 A) completely prevented this decrease in the cross-sectional area (Fig. 4, B and C).

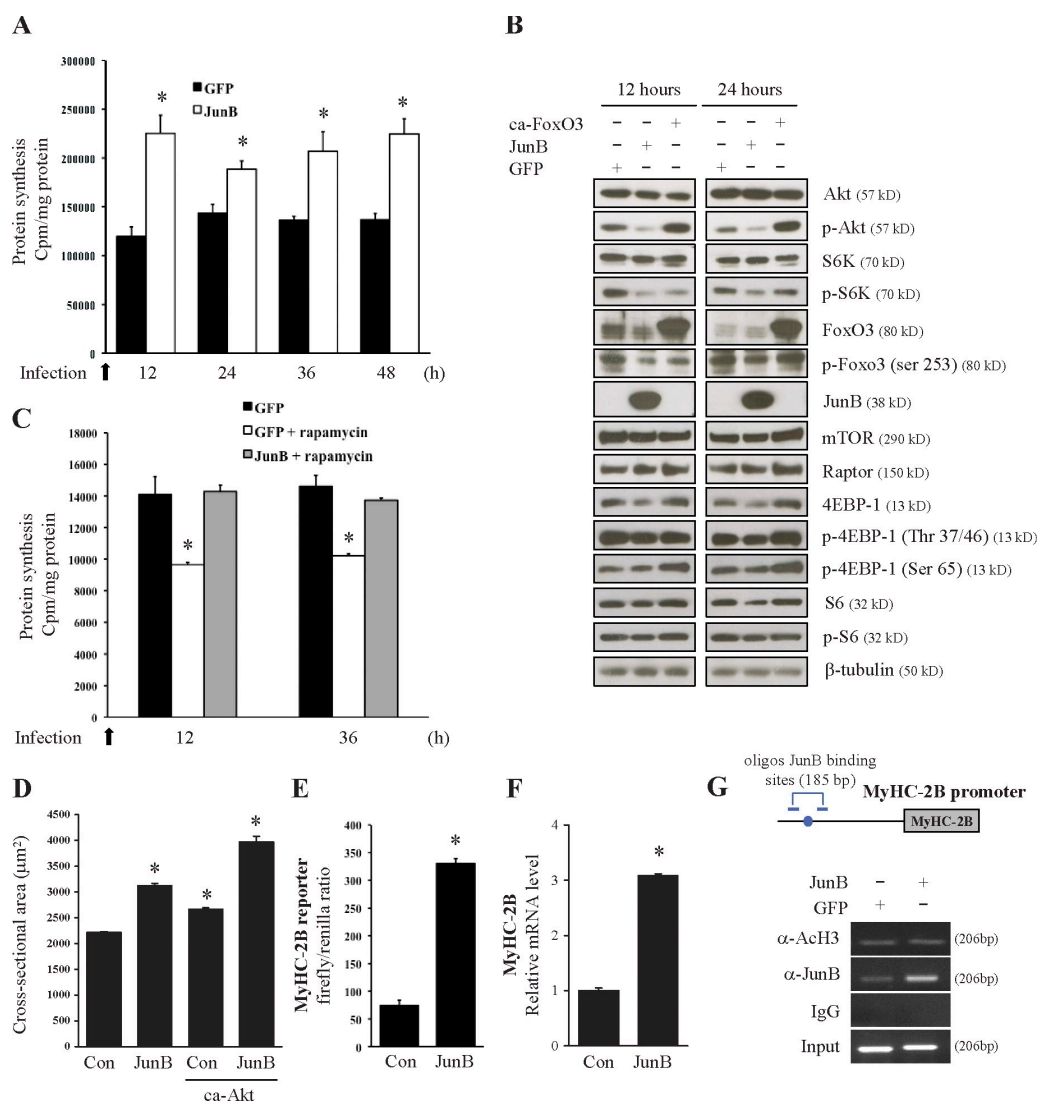


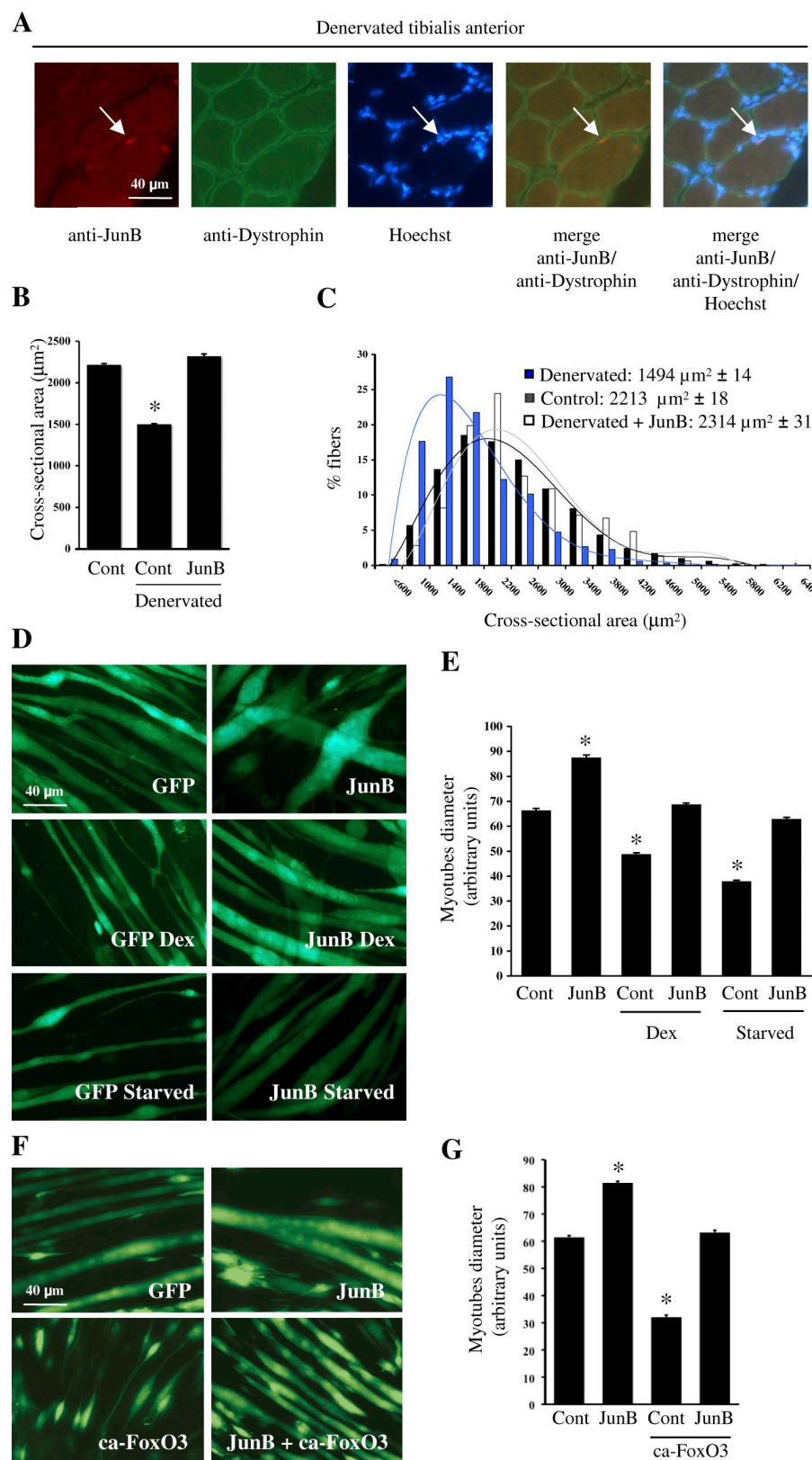
Figure 3. JunB promotes rapid muscle fiber growth by increasing protein synthesis independently of the Akt/mTOR pathway. (A) JunB enhances protein synthesis in differentiated myotubes. At different times after infection with adenoviruses expressing JunB or GFP (mock plasmid), cells were incubated with [³H]tyrosine for 2 h. The radioactivity incorporated, normalized to total protein, was determined. (B) The effects of JunB and ca-FoxO3 on phosphorylation of components of the AKT pathway are depicted. Differentiated myotubes were infected for 12 and 24 h with either mock (GFP), JunB, or ca-FoxO3 adenovirus. Immunoblot analysis with specific antibodies was performed. (C) JunB stimulates protein synthesis in differentiated myotubes even in the presence of rapamycin. C2C12 myotubes were infected with control GFP- or JunB-expressing adenoviruses with or without rapamycin. The experiment was performed as in A. (A and C) $n = 6$; means \pm SD. *, $P < 0.01$. (D) Overexpression of JunB in TA muscles of Akt transgenic mice stimulates further hypertrophy. Adult muscles of transgenic animals expressing activated Akt under control of tamoxifen (Mammucari et al., 2007) were transfected with a plasmid expressing JunB for 9 d. Akt was activated by tamoxifen injection immediately after electroporation. The bar diagram represents the mean cross-sectional area of at least 500 control fibers expressing Akt and of the same number of fibers coexpressing JunB \pm SEM. $n = 3$. *, $P < 0.01$. (E) Effect of JunB on the activity of the myosin heavy chain type 2B (MyHC-2B) promoter. Mouse TA muscles were electroporated with MyHC-2B promoter, driving the firefly luciferase gene and the control vector pRL-TK with or without JunB for 9 d. The values represent the firefly activity normalized to renilla luciferase activity. $n = 3$; means \pm SD. *, $P < 0.01$. (F) Effect of the overexpression of JunB on MyHC-2B mRNA. C2C12 myotubes were infected with either JunB or GFP adenoviruses. At different time points, cells were collected, and total RNA was analyzed by quantitative RT-PCR. $n = 3$; means \pm SD. *, $P < 0.005$. (G) JunB induces the expression of MyHC-2B by direct binding to its promoter. Differentiated myotubes were infected with either mock (GFP) or JunB adenoviruses. After 48 h, ChIP was performed using anti-JunB and anti-acetyl histone antibodies. A set of primers that cover the JunB response elements of the MyHC-2B promoter was used to amplify by PCR the related DNA fragments on the MyHC-2B promoter as depicted in the top panel.

A similar inhibition of atrophy was observed in myotubes under catabolic conditions. Both nutrient removal and dexamethasone treatment caused myotube atrophy (Fig. 4 D; Sandri et al., 2004), and JunB overexpression completely prevented these decreases of myotube size (Fig. 4, D and E). Because catabolic stimuli activate FoxO transcription factors, we also used a genetic approach to activate the atrophy program in myotubes. It is known that the overexpression of constitutively active FoxO3

(ca-FoxO3) in myotubes causes dramatic fiber atrophy (Sandri et al., 2004; Zhao et al., 2007). However, JunB overexpression (Fig. 4 F) together with ca-FoxO3 completely prevented the FoxO-mediated atrophy (Figs. 4, F and G and S4 B).

To clarify the mechanisms for this dramatic prevention of atrophy, we investigated whether JunB overexpression in atrophying muscles and myotubes affects the induction of the critical atrophy-linked ubiquitin ligases atrogin-1 and MuRF-1

Figure 4. JunB blocks fiber atrophy induced by denervation of TA muscles and myotube atrophy induced by *ca-FoxO3*, treatment with dexamethasone, and starvation. (A–C) JunB counteracts the decrease in fiber size upon denervation. JunB was electroporated into TA muscles of adult mice, and, at the same time, the left hindlimb was denervated. 9 d after denervation, the TA muscles were analyzed by immunohistochemistry. (A) JunB and dystrophin staining demonstrates that JunB-positive nuclei lay under the sarcolemma. The arrows indicate the myonuclei overexpressing JunB. (B) Cross-sectional area of at least 500 transfected fibers identified by anti-JunB immunofluorescence was measured as previously described and compared with an equal number of untransfected denervated fibers and control innervated fibers \pm SEM. $n = 4$. *, $P < 0.001$. (C) Frequency histograms showing the distribution of cross-sectional areas of ~ 500 denervated fibers (light blue bars), of ~ 500 denervated fibers expressing JunB for 9 d (open bars), and an equal number of innervated fibers (control fibers; shaded bars). The numeric data are expressed as the mean fiber sizes \pm SEM. $n = 4$. (D and E) JunB increases the size of differentiated myotubes and blocks myotube atrophy induced by dexamethasone and starvation. 5-d differentiated myotubes were infected with adenoviruses expressing mock (GFP) and JunB. (D) The panels show the myotubes 48 h after infection. The myotubes expressing control GFP and JunB were then treated with dexamethasone or starved. (E) The bar diagram represents the mean diameter of at least 1,000 myotubes infected with mock (GFP) or JunB adenoviruses untreated or treated with dexamethasone or starved \pm SEM. $n = 3$. *, $P < 0.001$. (F and G) JunB increases the size of differentiated myotubes and counteracts FoxO3-induced atrophy. 5-d differentiated myotubes were infected with adenoviruses expressing mock (GFP), JunB, *ca-FoxO3*, and *ca-FoxO3* together with JunB. (F) The panels show the myotubes 48 h after infection. (G) Mean diameter of myotubes infected with mock (GFP), JunB, *ca-FoxO3*, and JunB together with *ca-FoxO3* adenoviruses. The experiment was performed as in E. *, $P < 0.001$. Means \pm SEM.



using promoter reporter constructs (Bodine et al., 2001a; Gomes et al., 2001; Lecker et al., 2004; Sacke et al., 2007). Importantly, JunB overexpression in the denervated muscles prevented the activation of the atrogen-1 promoter (Fig. 5 A) and greatly reduced that of MuRF-1 (Fig. 5 B). Consistent with the in vivo

data, overexpression of JunB in myotubes (Fig. S4 A) completely blocked atrogen-1 induction (Fig. 5 C) and partially inhibited that of MuRF-1 (Fig. 5 D) during dexamethasone treatment and nutrient deprivation, both of which induce myotube atrophy and induction of atrogen-1 and MuRF-1 (Sandri et al., 2004).

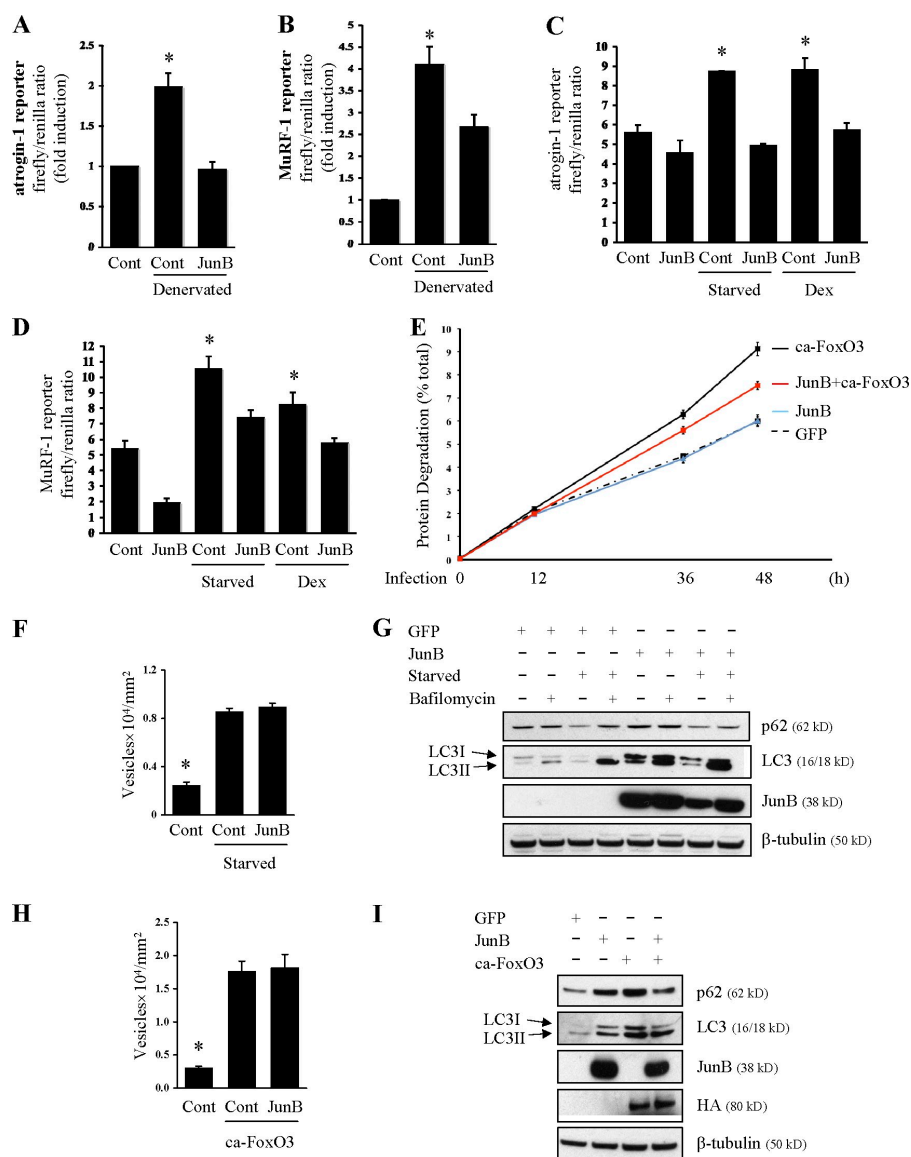


Figure 5. JunB greatly reduces the induction of the critical atrophy-related ubiquitin ligases atrogin-1 and MuRF-1 in TA muscles and in myotubes in atrophying conditions and reduces the increase in overall proteolysis induced by ca-FoxO3. (A and B) JunB overexpression in TA muscles blocks the induction of atrogin-1 (A) and inhibits the induction of MuRF-1 (B) after denervation. Muscles were cotransfected with atrogin-1 or MuRF-1 promoter with pRL-TK in the presence or absence of JunB. After 6 d, the muscles were denervated unilaterally by cutting the sciatic nerve to induce the expression of these two ubiquitin ligases. 2 d later, the muscles were collected, and the firefly/renilla luciferase ratio was determined as described in Fig. 3 E. $n = 4$; means \pm SD. (C and D) Overproduction of JunB inhibits the induction of atrogin-1 (C) and MuRF-1 (D) promoters in C2C12 myotubes starved or treated with dexamethasone. C2C12 myoblasts were transfected with atrogin-1 (Sandri et al., 2004) or with MuRF-1 promoters with or without JunB. A renilla luciferase construct (pRL-TK) was cotransfected to normalize for transfection efficiency. 5-d differentiated myotubes were starved or incubated with dexamethasone as in Fig. 1 A. The expression of atrogin-1 and MuRF-1 promoters was determined by firefly activity and normalized for the renilla. $n = 3$; means \pm SD. (A–D) *, $P < 0.01$. (E) JunB reduces the increase in overall proteolysis induced by FoxO3. To label cell proteins, differentiated myotubes were incubated with [3 H]tyrosine for 20 h as described previously (Zhao et al., 2007). Cells were then infected with mock (GFP), ca-FoxO3, or JunB adenoviruses. Media samples were collected over 48 h. Proteolysis was measured as described previously (Zhao et al., 2007). $n = 6$; means \pm SD. (F–I) JunB does not affect autophagosome formation induced by starvation and ca-FoxO3. (F) Adult TA muscles were transfected with a plasmid expressing YFP-LC3 with or without JunB. 9 d later, mice were fasted for 24 h before sacrifice. Myofibers expressing YFP-LC3 were analyzed by fluorescence microscopy, and cryosections were stained for JunB. Autophagosomes were quantified as described

previously (Mammucari et al., 2007). (G) Differentiated myotubes were infected with mock (GFP) or JunB adenoviruses for 48 h and then starved and treated with bafilomycin A for 5 h to inhibit lysosomes. Proteins were extracted, and LC3 lipidation was determined by the extent of conversion of LC3I to LC3II. (H) Adult TA muscles were transfected with a plasmid expressing YFP-LC3 with or without JunB and ca-FoxO3. 9 d later, mice were sacrificed, and autophagosomes were analyzed as in F. (F and H) $n = 4$; means \pm SEM. *, $P < 0.001$. (I) Differentiated myotubes were infected with either mock (GFP), JunB, ca-FoxO3, or JunB with ca-FoxO3 adenoviruses for 48 h. Proteins were extracted and analyzed as in G. The HA line represents ca-FoxO3 expression because ca-FoxO3 is HA tagged.

Quantitative RT-PCR confirmed that JunB overproduction markedly decreased the levels of mRNA for these two ligases in untreated myotubes (Fig. S5, A and B). Thus, maintenance of high levels of JunB in catabolic conditions preserves muscle mass and blocks the atrophy program.

JunB inhibits the activation of proteolysis by FoxO3

The FoxO family of transcription factors plays a critical role in muscle atrophy upon denervation, and FoxO3 activation by itself can induce rapid atrophy as well as *atrogin-1* and *MuRF-1* expression (Sandri et al., 2004) and stimulate proteasomal and autophagic/lysosomal proteolysis (Mammucari et al., 2007; Zhao et al., 2007). We therefore tested whether JunB could

also inhibit this stimulation of overall protein degradation by FoxO3. After labeling the bulk of cell proteins in myotubes with [3 H]tyrosine for 20 h (Zhao et al., 2007), the rate of degradation of long-lived proteins was measured in C2C12 myotubes after infection with adenoviruses bearing the JunB, FoxO3, or a mock (GFP) construct. As shown previously (Zhao et al., 2007), ca-FoxO3 expression stimulated overall proteolysis in myotubes above rates in control myotubes (Fig. 5 E). Overexpression of JunB alone did not change the basal rate of protein degradation, which supports our earlier conclusion that JunB stimulates growth of normal fibers (Fig. 2, B and C) by stimulating protein synthesis (Figs. 3 A and S2 B). However, JunB partially inhibited the rise in proteolysis caused by ca-FoxO3 (Fig. 5 E). These findings are in accord with our finding that JunB suppresses the

activation of the atrogin-1 and MuRF-1 promoters (a FoxO3-mediated effect) in atrophying muscles (Fig. 5, A and B).

Because the induction of protein breakdown by ca-FoxO3 was only partially reduced, we monitored whether JunB also prevents the activation of the autophagic/lysosomal pathway by ca-FoxO3 or by fasting. Adult skeletal muscles were transfected with a YFP-LC3 plasmid to monitor autophagosome formation. Overexpression of JunB *in vivo* did not prevent autophagic vesicle formation in FoxO3-transfected TA or TA of fasted mice, as revealed by the number of LC3-positive punctae (Fig. 5, F and H). Consistently, JunB overexpression also did not block the LC3 lipidation during starvation or FoxO3 overexpression (Fig. 5, G and I). We have shown that FoxO3 activates autophagy by regulating the expression of several autophagy-related genes, including *Bnip3* and *Beclin-1* (Mammucari et al., 2007; Zhao et al., 2007), and the induction of *Bnip3* and *Beclin-1* is sufficient for induced autophagosome formation (Mammucari et al., 2007). Interestingly, JunB did not prevent the FoxO3-mediated induction of these two genes (Fig. S5 C). Thus, JunB does not decrease basal protein breakdown in muscle but can specifically reduce the stimulation of proteasomal-dependent protein degradation by FoxO3 (Fig. 5 E). This finding also supports our earlier conclusion that JunB does not act through the Akt/mTOR signaling pathway (Figs. 3, B–D and S3 C), whose activation suppresses basal protein degradation (Sacheck et al., 2007).

JunB interacts with FoxO3 and inhibits its binding to the atrogin-1 promoter

To clarify the mechanism by which JunB reduces the induction of atrogin-1 and MuRF-1, the stimulation of proteolysis by ca-FoxO3, and the loss of muscle mass, we tested by ChIP the ability of JunB to inhibit FoxO3 binding to the atrogin-1 promoter in myotubes infected either with JunB or JunB together with ca-FoxO3 adenoviruses. As predicted, JunB overproduction in C2C12 myotubes strongly reduced the binding of FoxO3 to its specific recognition sequences on the promoter (Fig. 6 A, left). In the same myotubes, we also tested the ability of JunB to interact with specific AP-1 binding sequences on the atrogin-1 promoter, and indeed we confirmed that this factor binds to the promoter of this crucial ubiquitin ligase (Fig. 6 A, right).

Interestingly, one of the AP-1 binding sites in the atrogin-1 promoter lies close to the FoxO binding site (Fig. 6 A), and it seemed likely that JunB might interact with this AP-1 site and thereby might inhibit the binding of FoxO3 to this promoter. To examine this possibility, we cloned this promoter region upstream of the luciferase gene and then mutagenized the AP-1 site. FoxO3 was able to induce the two reporters, the wild type and the mutated one (Fig. 6 B), and, surprisingly, JunB coexpression was still able to block FoxO3's action on both promoters (Fig. 6 B). Furthermore, this inhibition of both promoters by JunB did not require the presence of its DNA-binding domain (Fig. 6 B). Thus, this important ability of JunB to inhibit FoxO activity does not require JunB binding to the atrogin-1 promoter. FoxO activity is regulated not only by multiple posttranslational modifications (including acetylation, ubiquitination, and phosphorylation) but also by interactions with other proteins (Calnan and Brunet, 2008; van der Vos and Coffey, 2008). To test whether

this inhibition of FoxO actions could be the result of a direct interaction of JunB with FoxO3, we performed a coimmunoprecipitation experiment in myotubes infected with the control plasmid (GFP), JunB, ca-FoxO3, or both JunB and ca-FoxO3. This experiment clearly demonstrated that JunB forms a complex with FoxO3 (Fig. 6 C, top). The JunB–FoxO3 interaction was also confirmed by immunoprecipitating the endogenous proteins (Fig. 6 C, bottom). Together, these results indicate that JunB associates with FoxO3 to directly block its recruitment to the atrogin-1 and MuRF-1 promoters and thus inhibits muscle atrophy.

Because JunB induction of hypertrophy is independent of Akt signaling, we monitored whether JunB might influence the myostatin pathway. In fact, we have recently shown that myostatin inhibition induces hypertrophy in adult myofibers (Sartori et al., 2009). Interestingly, JunB overexpression greatly suppressed *myostatin* expression in transfected myotubes (Fig. 6 D). Because a prior study has shown that JunB is downstream of TGF- β /small mother against decapentaplegic (Smad) signaling (Li et al., 1990), we also monitored whether myostatin treatment could modulate *JunB* expression. However, at two different concentrations tested, myostatin was unable to change the level of *JunB* transcript (Fig. 6 E). To further confirm that JunB can block myostatin signaling, we monitored Smad3 phosphorylation, the transcription factor downstream of myostatin. FoxO1 has, in fact, been shown to control *myostatin* expression (Allen and Unterman, 2007). Indeed, FoxO3 expression induced Smad3 phosphorylation (Fig. 6 F). Conversely, JunB overexpression caused dephosphorylation of Smad3, confirming the inhibitory effect on *myostatin* expression (Fig. 6 F), and this effect probably contributes to the muscle growth induced by JunB.

Discussion

Although it is well established that JunB is of fundamental importance in regulating cell proliferation (Bakiri et al., 2000; Passequé and Wagner, 2000), including proliferation of muscle cell progenitors (Chalaux et al., 1998), and also appears to suppress growth of certain tumors, few studies have addressed the role of JunB or other AP-1 family members in postmitotic cells. Our findings show that JunB, but not c-Jun, is a potent regulator of muscle mass in adult animals. Several studies have suggested that the activity of the AP-1 family is finely regulated in skeletal and cardiac muscles. For example, the expression of some of the members of this family, including JunB, can be induced by exercise (Trenerry et al., 2007) or insulin (Coletta et al., 2008), and JunB mRNA rises during cardiac hypertrophy induced by increased workload (Black et al., 1991), β agonists (Brand et al., 1992), and electrical stimulation (Xia et al., 1997). These observations are consistent with our findings that JunB expression falls during various types of atrophy (Lecker et al., 2004; Sacheck et al., 2007), that JunB is excluded from the nucleus in atrophying myotubes (Fig. 1 A), and that the AP-1 binding to DNA sharply decreases during starvation of myotubes (Sandri et al., 2004). Furthermore, we found that the endogenous expression of JunB in normal muscles is required for the maintenance of muscle mass in adult animals. In fact, the decrease of JunB content (Fig. 1 C) leads to rapid decreases in fiber diameter (Fig. 1, D and E).

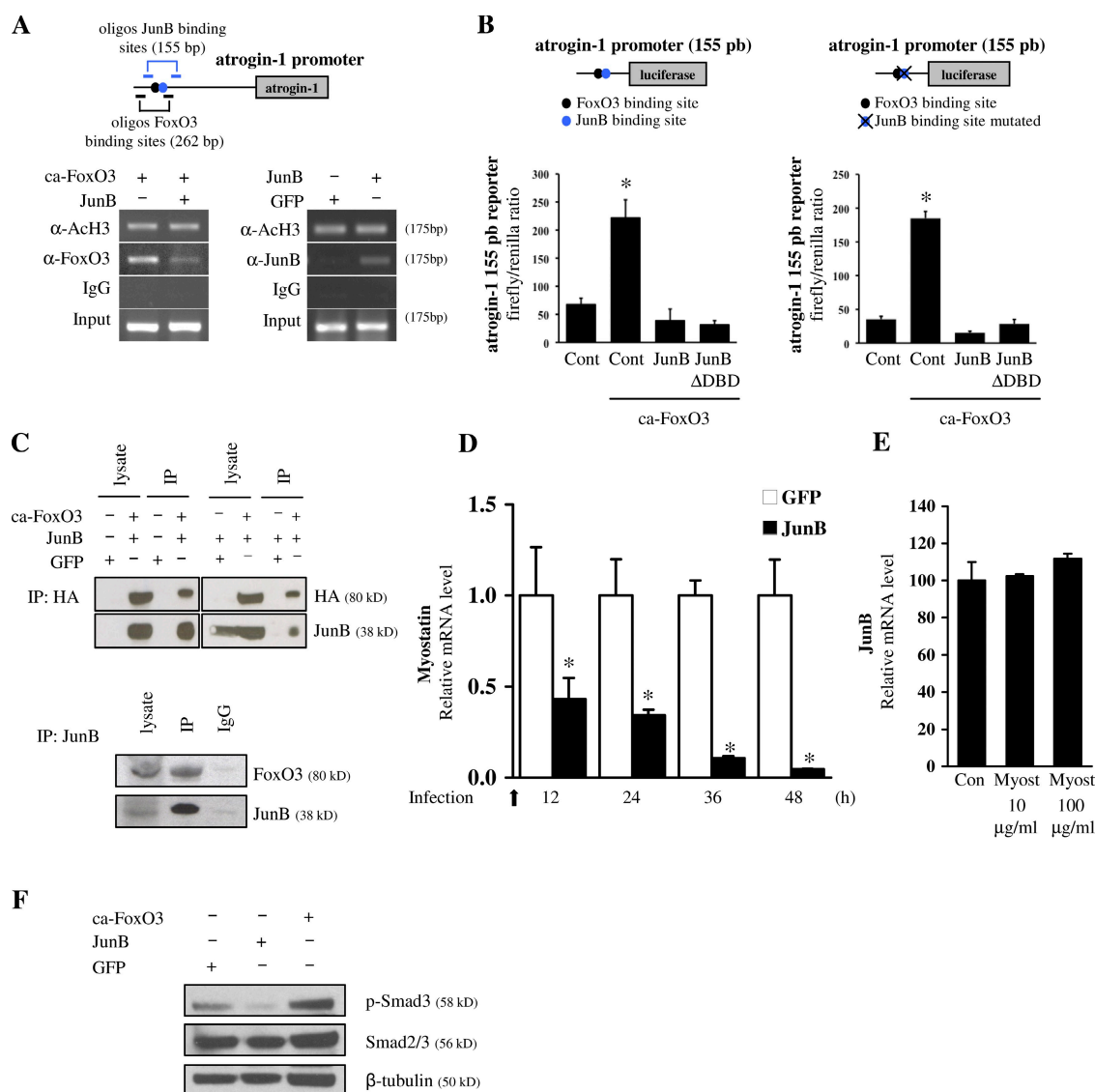


Figure 6. JunB interacts with FoxO3, prevents its binding to the atrogin-1 promoter, and inhibits the activity of the myostatin/Smad pathway. (A) JunB inhibits the recruitment of FoxO3 to the atrogin-1 promoter. Differentiated myotubes were infected with either mock (GFP), JunB, ca-FoxO3, or ca-FoxO3 and JunB adenoviruses. 48 h later, ChIP was performed using an anti-FoxO3, an anti-JunB, and anti-acetyl histone-specific antibodies. A set of primers that cover the JunB and FoxO3 response elements of the atrogin-1 promoter were used to amplify by PCR the related DNA fragments on the atrogin-1 promoter as depicted in the top panel. (B) FoxO3 recruitment on the atrogin-1 promoter is blocked by JunB independently of the AP-1 binding site. A plasmid coding for the region of the atrogin-1 promoter (155 bp) containing the FoxO and AP-1 sites (or the mutated one) linked to a minimal SV40 promoter and a luciferase reporter was transfected into adult TA muscles in the presence or absence of ca-FoxO3, wild-type JunB (JunB), or a JunB mutant lacking the DNA-binding domain (JunB ΔDBD) with the renilla luciferase construct (pRL-TK) to normalize for transfection efficiency. 6 d later, firefly/renilla luciferase activity was determined. $n = 4$; means \pm SD. (C) JunB interacts with FoxO3. (top) Differentiated myotubes were infected with adenoviruses expressing either mock (GFP), JunB, or JunB and ca-FoxO3. 2 d later, HA-tagged FoxO3 was immunoprecipitated from cell proteins with a specific anti-HA antibody. The immunoprecipitated proteins were immunoblotted with anti-HA and JunB antibodies. (bottom) Endogenous JunB was immunoprecipitated from C2C12 myotubes using the anti-JunB-specific antibody. The eluted proteins were assayed by immunoblotting and visualized with anti-FoxO3 and anti-JunB antibodies. (D) JunB inhibits myostatin expression in differentiated myotubes. C2C12 myotubes were infected with either mock (GFP) or JunB adenoviruses for 12, 24, 36, and 48 h. Myostatin expression was assessed by quantitative RT-PCR. (B and D) *, $P < 0.001$. (E) Myostatin treatment does not influence JunB expression in differentiated myotubes. Adult myotubes were treated with either 10 or 100 μ g/ml myostatin for 2 d and analyzed by quantitative RT-PCR. (D and E) $n = 3$; means \pm SD. (F) JunB inhibits Smad3 phosphorylation in myotubes. Differentiated myotubes were infected with mock (GFP), JunB, and ca-FoxO3-specific adenoviruses. 24 h later, the cells were collected, and proteins were immunoblotted with specific antibodies for phospho-Smad3 and total Smad2/3.

Thus, it is likely that the fall in JunB expression (Lecker et al., 2004; Sacheck et al., 2007) and its exclusion from the nucleus in atrophying muscles (Fig. 1 A) contribute to the loss of muscle protein in various catabolic conditions. In particular, based on JunB's ability to stimulate muscle protein synthesis and myosin expression, their fall in catabolic (i.e., JunB deficient) states is likely to be caused, at least in part, by the reduced JunB activity.

JunB overexpression leads to dramatic hypertrophy of both myotubes (Fig. 4, D and F) and adult mouse muscles (Fig. 2) by stimulating overall protein synthesis (Fig. 3 A) and myosin expression (Fig. 3, E and F), and, surprisingly, JunB does so without activating the mTOR/S6K pathway (Fig. 3, B–D) and without reducing basal protein degradation (Fig. 5 E). We have recently shown that inhibition of the TGF- β pathway also

promotes muscle growth by an Akt-independent mechanism (Sartori et al., 2009). Indeed, JunB blocks *myostatin* expression and thus inhibits the TGF- β /Smad pathway. How much of JunB's growth-promoting effect is mediated via *myostatin* inhibition is an interesting point that merits more detailed investigations. Alternatively, JunB and decreased myostatin activity may enhance protein synthesis via related mTOR-independent mechanisms, such as increasing translational efficiency or ribosome content. Importantly, the prevention of denervation atrophy by JunB (Fig. 4, A–C) cannot be ascribed solely to the inhibition of FoxO3 activity because its overexpression did not completely abolish FoxO3-mediated protein breakdown (Fig. 5 E). Therefore, other JunB actions (e.g., its stimulation of protein synthesis) must be crucial in inducing such rapid growth of normal muscle, whereas JunB's ability to prevent fiber atrophy upon denervation (Fig. 4, A–C) must reflect a combination of different actions, including the enhancement of synthesis (Fig. 3 A) together with JunB's interaction with FoxO to inhibit the activation of proteolysis (Fig. 5 E).

Although Akt activation and JunB expression can both prevent FoxO3 binding to the promoters of atrogen-1 and MuRF-1 and the induction of these (and presumably certain other) atrogenes, Akt and JunB do so by very different mechanisms and to different extents. Akt phosphorylates FoxO3 and thereby prevents its migration to the nucleus (Sandri et al., 2004). In contrast, JunB associates with FoxO3 (Fig. 6 C) and thus reduces FoxO3 recruitment to promoters of key atrogenes (Fig. 6, A and B). Akt and JunB also seem to have distinct effects on protein degradation. When activated, Akt causes a general reduction in protein degradation in normal and atrophying muscles and myotubes (Zhao et al., 2007) by suppressing autophagy through mTOR stimulation and by inactivating FoxO3, which prevents the activation of both the autophagic/lysosomal and the ubiquitin–proteasomal pathways. In contrast, JunB lowers only the accelerated proteolysis induced by activated FoxO3 but does not block the activation of autophagy by FoxO3 (Fig. 5, F–I). Because JunB overexpression can prevent completely the loss of muscle mass upon denervation (Fig. 4, A–C), JunB, by binding to FoxO3, appears to reduce its capacity to cause atrophy-related gene induction and probably also stimulates protein synthesis.

Presently, no therapies are available to combat the debilitating loss of muscle in bed-ridden patients during acute systemic diseases (e.g., cancer, sepsis, or neurodegenerative disease) or in the frail elderly. Because increasing JunB can cause marked hypertrophy and can block the rapid loss of muscle mass upon denervation or by FoxO3 activation, raising or maintaining JunB levels represents a potential new therapeutic target for the development of drugs that ameliorate the muscle wasting that accompanies many systemic diseases.

Materials and methods

Cell culture, adenoviral infection, and measurement of myotube diameter
C2C12 myoblasts (American Type Culture Collection) were cultured in DME + 10% FBS (Invitrogen) until cells reached confluence. The medium was then replaced with DME + 2% horse serum (Invitrogen) and incubated for 5 d before proceeding with experiments. For infection, 5-d differentiated myotubes were incubated with adenovirus at an MOI of 250 in

differentiation medium and treated with 100 μ M dexamethasone (Sigma-Aldrich) or with PBS for 5 h with 10 or 100 μ g/ml myostatin (R&D Systems) as previously described (Trendelenburg et al., 2009) and with 200 nM bafilomycin A (LC Laboratories) for 5 h as previously described (Romanello et al., 2010). Experiments were performed on an inverted microscope (IX81; Olympus) with the UPlan FLN 20 \times /0.5 NA objective (Olympus). The microscope was equipped with a charge-coupled device camera (SIS F-View; Olympus), an illumination system (MT20; Olympus), and a beam-splitter optical device (Multispec Microimager; Optical Insights). Images were collected using Cell-R software (Olympus). The cells were fixed with 4% PFA for 10 min and maintained in PBS solution at room temperature. Myotube diameter was measured in \sim 1,000 myotubes for each condition using IMAGE software (Scion Corporation). All the data are expressed as means \pm SEM. Comparisons were made using the Student's *t* test with *P* < 0.05 being considered statistically significant.

The infection efficiency was typically >90%. Adenoviruses expressing ca-FoxO3 and GFP were described previously in Skurk et al. (2004).

Adenovirus production

The adenovirus expressing JunB was created using the AdEasy strategy (Agilent Technologies). Human JunB cDNA was cloned in the pAdTrack cytomegalovirus vector (Agilent Technologies). Subsequent steps were performed according to the manufacturer's instructions. Adenoviral vectors contain two distinct promoters that independently drive the expression of the gene of interest and of GFP. Therefore, mock plasmid expresses only GFP.

Plasmids

The expression plasmid for wild-type JunB was provided by J.S. Brugge (Harvard Medical School, Boston, MA). The JunB mutant lacking the DNA-binding domain was created by the deletion of 21 amino acids (amino acids 249–270) by mutagenesis PCR using the wild-type JunB expression vector as a template and the mutagenesis primer 5'-CAGACCGTCCGGAGGCGGTGGAGCGCAAGCGGCTG-3'. The expression vector coding for c-Jun was provided by J. Blenis (Harvard Medical School, Boston, MA).

The reporter construct containing 155 bp of the atrogen-1 promoter (from –3,088 to –2,933) driving the firefly luciferase gene was created by PCR with the oligonucleotide primers used also for the ChIP experiments and inserted into the KpnI and XhoI sites of pGL3-Promoter Vector (Promega). The oligonucleotide primers used for the PCR reaction are forward 5'-TCCCTGCAGGATGAAATGT-3' and reverse 5'-GTATGCCCTGGGTCCAAGT-3'.

Mutations in the AP-1 binding site were generated by PCR using the QuickChange technique (Agilent Technologies). The oligos (AP-1 site is in bold and the mutated nucleotides are underlined) used are atrogen-1 wild type (5'-CAAACAAGATTTTCCCAATTCCT**GAGT**CAAAATTGGAGACGGCTTTGCC-3') and atrogen-1 mutated (5'-CAAACAAGATTTTGC-CAATTCCT**GCGC**AAATTGGAGACGGCTTTGCC-3').

Transient transfection and luciferase assays in muscle cell cultures

Myoblasts were transfected with different reporters using Lipofectamine 2000 (Invitrogen) according to the manufacturer's instructions. Generally, 100 \times 10³ C2C12 cells were seeded into individual wells of 12-well plates 24 h before transfection with either 3.5 kb of atrogen-1 promoter (3.5 AT1) or 5 kb of MuRF-1 promoter (5.0 MuRF-1) reporter constructs and pRL-TK (Promega) with or without either JunB or ca-FoxO3 expression vectors (2 μ g of total DNA/well, 0.5 μ g of reporter, 0.5 μ g pRL-TK, 1 μ g JunB expression vector, and 1 μ g ca-FoxO3 expression vector). When the cells reached confluence, the medium was shifted to differentiation medium to induce myotube formation. After 5 d, myotubes were treated either with 10 μ M dexamethasone for 24 h or with PBS for 5 h. After these treatments, myotubes were lysed and analyzed using the Dual-Luciferase Reporter Assay System (Promega) according to the manufacturer's instructions. To control for transfection efficiency, firefly luciferase activity was divided by renilla luciferase activity. Luciferase measurements in muscles transfected with reporter constructs were performed similarly, except that the harvested muscles were quick frozen and powdered in liquid nitrogen before the addition of the lysis buffer (Serrano et al., 2001). Results are expressed as means \pm SD of at least three independent experiments.

Adult mouse skeletal muscle transfection and treatments

Adult male CD1 mice (2 mo of age) were used in all overexpression experiments. In the RNAi experiments, adult male CD1 mice (3 mo of age) were used. TA muscles were transfected as described previously (Donà et al., 2003). The muscle was isolated through a small hindlimb incision, and 20 μ g of plasmid DNA was injected along the muscle length. In the reporter experiments, 20 μ g of the expression vector with 10 μ g of either 2.8 MyHC-2B,

3.5 AT1 or 5.0 MuRF-1 or 155 bp atrogen-1 promoter reporter constructs and 5 µg pRL-TK vectors were coinjected. Electric pulses were then applied by two stainless steel spatula electrodes placed on each side of the isolated muscle belly (21 V/cm for five pulses at 200-ms intervals). For the determination of the number of autophagic vesicles, mouse TA muscles of 2-mo-old mice were electroporated with YFP-LC3 expression plasmid and starved for 24 h as previously described (Mammucari et al., 2007). JunB overexpression experiments were performed on 2-mo-old mice. Electroporated muscles were collected 6, 9, or 12 d later. No gross or microscopic evidence for necrosis or inflammation as a result of the transfection procedure was noted. For the BrdU experiments, CD1 mice were electroporated with the JunB expression vector. BrdU was injected every day starting from day 5 after transfection until the animal was sacrificed. Every injection contained 50 mg/kg BrdU dissolved in 100 µl of 0.9% NaCl. Satellite cell activation and muscle regeneration were induced by injection in TA muscles of 10 µl of 35-µM cardiotoxin (Sigma-Aldrich). For the inhibition of protein synthesis, *in vivo* CD1 mice were injected subcutaneously every day for 5 d with 15 mg/kg cycloheximide (Sigma-Aldrich) dissolved in 0.9% NaCl as previously described (Fan et al., 2010).

Immunohistochemistry, fiber size measurements, and determination of the number of autophagic vesicles

10-µm-thick cryosections of muscles overexpressing either JunB or c-Jun for 9 d were fixed by 4% paraformaldehyde. Immunohistochemistry with either an anti-JunB polyclonal antibody (Santa Cruz Biotechnology, Inc.) or an anti-c-Jun polyclonal antibody (Abcam) was performed as previously described (Sandri et al., 2004; Mammucari et al., 2007; Sartori et al., 2009). Muscle fiber size was measured in fibers expressing JunB or c-Jun and in equal numbers of untransfected fibers from the same muscle as previously described (Mammucari et al., 2007; Sartori et al., 2009). Cryo-cross sections were also stained with antidystrophin-specific antibodies (Sigma-Aldrich and Abcam).

Inducible muscle-specific Akt transgenic mice are described in Mammucari et al. (2007). Transgenic animals were electroporated with the JunB expression vector and, immediately after the electroporation, were injected with 1.5 µg tamoxifen (Sigma-Aldrich) to induce the expression of Akt (Mammucari et al., 2007). The treatment was repeated every other day to maintain Akt expression for the duration of the experiment. Control animals received only oil vehicle. After 9 d from the electroporation of JunB, the muscles were collected, and transfected fibers were revealed by immunohistochemistry with specific antibodies against JunB. Cross-sectional area was measured in fibers overexpressing JunB and compared with an equal number of surrounding untransfected fibers.

For the determination of the number of autophagic vesicles, cryosections of muscle transfected with YFP-LC3 expression plasmid were examined using a fluorescence microscope, and fluorescent dots were counted as described previously, normalizing for cross-sectional area (Mizushima et al., 2004; Mammucari et al., 2007).

To identify BrdU-positive nuclei, 4–6-µm cryostat sections were incubated with 4 M HCl and trypsin to expose the DNA to the antibody as previously described (Sartori et al., 2009). The antibody against BrdU-FITC conjugate was purchased from Abcam, and the antibody anti-laminin was obtained from Sigma-Aldrich. All fiber cross-sectional areas were measured using IMAGE software. Slides were mounted with Elvanol (Sigma-Aldrich) and analyzed with a microscope (DM5000B; Leica) using an HCPL Fluotar 20x/0.5 NA objective lens (Leica). Images were collected with a camera (DFC300FX; Leica) and analyzed with IM50 Image software (Leica).

All the data are expressed as means ± SEM. Comparisons were made using the Student's *t* test with *P* < 0.05 being considered statistically significant.

Protein degradation measurement in C2C12 myotubes

C2C12 myotubes were incubated with 5 µCi/ml [³H]tyrosine for 20 h to label cell proteins and then were switched to chase medium (containing 2 mM of unlabeled tyrosine to prevent reincorporation of [³H]tyrosine; Gronostajski et al., 1984) for 2 h. Fresh chase medium containing GFP, JunB, ca-FoxO3, or JunB together with ca-FoxO3 adenoviruses was added, and media samples were collected over 32 h and combined with TCA (10% final concentration) to precipitate proteins. The acid-soluble radioactivity reflects the amount of prelabeled, long-lived proteins degraded at different times and was expressed relative to the total radioactivity initially incorporated. Plotting these values versus time gave the total rate of proteolysis. Results are expressed as means ± SD of six independent experiments.

Protein synthesis measurement in C2C12 myotubes

Total protein synthesis was measured by monitoring the incorporation of [³H]tyrosine into cell proteins according to the procedure of White et al. (1988). C2C12 myotubes were infected with GFP or JunB adenoviruses for 12, 24, 36, and 48 h, and, where indicated, the cells were treated for 12 and 36 h with 20 ng/ml rapamycin (LC Laboratories). Cells were then exposed to 5 µCi/ml [³H]tyrosine for 2 h. At the completion of the incubation period, the media were discarded. The wells were washed twice with PBS, and 1 ml of 10% TCA was added to each well to precipitate the proteins and incubated for 30 min at 4°C. Cells were removed from the plates using a rubber scraper and transferred to microfuge tubes. Tubes were spun for 5 min at 12,000 *g* at 4°C. The resulting pellet was washed with 1 ml of 95% ethanol. The pellet was solubilized in 1 ml of 0.1-M NaOH at 24°C for 2-h rocking. These samples were analyzed for both radioactivity and protein. For radioactivity measurements, 100 µl of each sample was transferred to a scintillation vial (Research Products International) with 3-ml scintillation cocktail (Ecolite; ICN Biomedicals, Inc.). Samples were mixed thoroughly and counted in a liquid scintillation counter (Packard Instruments). Total protein concentration was determined testing 50 µl of cellular material with the Bradford method (Thermo Fisher Scientific). Results were expressed as disintegrations per minute per milligram of protein for each well normalized on the control. Results are expressed as means ± SD of six independent experiments.

In vivo RNAi

In vivo RNAi experiments were performed as described previously (Sandri et al., 2004) using JunB siRNA (Invitrogen) to specifically knock down JunB. As a control, a nontargeting siRNA (scramble) was used (Invitrogen). The constructs are bicistronic vectors that encode shRNAs and GFP. Therefore, transfected fibers coexpress GFP together with the oligos. For the validation of siRNA constructs, murine embryonic fibroblasts were maintained in DME + 10% FBS (Invitrogen) and transfected with siRNA constructs using Lipofectamine 2000. Cells were lysed 72 h later, and proteins were purified and subjected to immunoblotting with specific antibodies against JunB.

Protein extraction and Western blotting

Total proteins were extracted by solubilization in lysis buffer (50 mM Tris, pH 7.5, 150 mM NaCl, 10 mM MgCl₂, 0.5 mM DTT, 1 mM EDTA, 10% glycerol, 2% SDS, 1% Triton X-100, 1 mM PMSF, 1 mM NaV, 5 mM NaF, 3 mM β-glycerol, and Complete EDTA-free protease inhibitor mixture [Roche]). Cytoplasmatic fraction from C2C12-differentiated myotubes was obtained with 10 mM Hepes, pH 7.6, 60 mM KCl, 1 mM EDTA, pH 8, and 0.1% NONIDET P-40. Nuclei were lysed with 20 mM Tris, pH 7.6, 420 mM NaCl, 1.5 mM MgCl₂, 0.2 mM EDTA, and 25% glycerol.

Protein concentration was quantified using the Bradford method. 30 µg of the whole-cell lysates and either the cytoplasmic or nuclear fraction was loaded and separated on 4–12% precast gels (Bis-Tris NuPAGE; Invitrogen). Proteins were transferred to Hybond-C Extra membrane (GE Healthcare) and stained with Ponceau S solution (Sigma-Aldrich) to verify the efficiency of the transfer. The blots were incubated in blocking buffer (TBS, 0.1% Tween 20, and 5% nonfat milk) for 1 h at room temperature. Membranes were washed in washing buffer (TBS and 0.1% Tween 20) three times for 5 min each, probed with the primary antibody in TBS, 0.1% Tween 20, and 2% nonfat milk overnight at 4°C, and then probed with the secondary antibody for 1 h in TBS, 0.1% Tween 20, and 2% nonfat milk. The antibody reaction was analyzed using the ECL method (Thermo Fisher Scientific).

The following antibodies from Cell Signaling Technology were used: anti-Akt, anti-phospho-Akt (Ser473), anti-phospho-FKHR1 (Ser253), anti-4EBP1, anti-phospho-4EBP1 (Ser65), anti-phospho-4EBP1 (Thr 37/46), anti-p70 S6 kinase, anti-phospho-p70 S6 kinase (Thr389), anti-S6, anti-phospho-S6 (Ser240/244), mTOR, and anti-phospho-Smad3 (Ser423/425). The following antibodies from Abcam were used: anti-JunB, anti-Raptor, anti-Fos, and anti-Fra1. The following antibodies from Santa Cruz Biotechnology, Inc. were used: anti-FKHR1, anti-β-tubulin, anti-GFP, anti-HDAC1, and anti-HA. The antibody anti-Smad2/3 was purchased from BD, the LC3 antibody was obtained from NanoTools, and the p62 antibody was purchased from PROGEN.

RNA extraction and gene expression analyses

Total RNA was purified from C2C12 myotubes infected either with GFP or JunB at different time points or from muscles transfected with scramble and JunB RNAi constructs for 12 d after the standard TRIZOL protocol (Invitrogen). The RNA was quantified and controlled for its quality using the RNA 6000 LabChip kit (Agilent Technologies) in conjunction with a 2100 Bioanalyzer (Agilent Technologies). Complementary DNA generated with a cDNA synthesis kit (SuperScript VILO; Invitrogen) was analyzed by quantitative real-time RT-PCR using the SYBR green chemistry (Finnzymes).

All data were normalized to glyceraldehyde-3-phosphate dehydrogenase expression. The following primers were used: glyceraldehyde-3-phosphate dehydrogenase forward (5'-ATACGGCTACAGCAACAGGG-3') and reverse (5'-TGTGAGGGAGATGCTCAGTG-3'); atrogen-1 forward (5'-TGGGTG-TATCGGATGGAGAC-3') and reverse (5'-TCAGCCTCTGCATGATGTC-3'); MuRF-1 forward (5'-CCTTCTCTCAAGTGCCAAAG-3') and reverse (5'-CCT-CAAGCCTCTGCTATGT-3'); JunB forward (5'-TCTCCTAAGGGAGCAA-GTGG-3') and reverse (5'-GGAGTCCAGTGTGTAGCTG-3'); MyHC-2B forward (5'-TAGGGTGAGGGAGCTGAAA-3') and reverse (5'-GTTTGT-CACCAAGTCTGC-3'); myostatin forward (5'-TGCAAAATGGCTCAAA-CAG-3') and reverse (5'-GCAGTCAAGCCCAAGTCTC-3'); LC3- β forward (5'-CACTGCTGTCTTGTAGGTG-3') and reverse (5'-TCGTTGTGC-CTTATTAGTCATC-3'); Gabarapl1 forward (5'-CATCGTGGAGAAGGCT-CCTA-3') and reverse (5'-ATACAGCTGGCCCATGGTAG-3'); Cathepsin L forward (5'-GTGGACTGTTCTACGCTCAAG-3') and reverse (5'-TCC-GTCTTCGCTTCATAGG-3'); beclin forward (5'-TGAATGAGGATGA-CAGTGAGCA-3') and reverse (5'-CACCTGGTTCTCCACACTCTTG-3'); and Bnip3 forward (5'-TTCCACTAGCACCTTCTGATGA-3') and reverse (5'-GAACACCGCATTACAGAACA-3').

Coimmunoprecipitation

C2C12 myotubes at the fourth day of differentiation were infected with either GFP, JunB, or JunB together with ca-FoxO3 adenoviruses. The cells were collected 2 d after the infection, and total proteins were extracted in an appropriate volume of lysis buffer (150 mM NaCl, 1% Triton X-100, 50 mM Tris-HCl, pH 7.5, and Complete EDTA-free protease inhibitor mixture). The coimmunoprecipitation was performed with the ProFound HA Tag IP/Co-IP kit (Thermo Fisher Scientific) because ca-FoxO3 is HA tagged. The eluted proteins were separated by SDS-PAGE gel electrophoresis, transferred to Hybond-C Extra membrane, and stained with Ponceau S solution. ca-FoxO3 was visualized with polyclonal anti-HA antibody (Santa Cruz Biotechnology, Inc.), and JunB was visualized with polyclonal anti-JunB antibody (Abcam). The immunoprecipitation of JunB to detect the interaction with Fos and Fra1 and the immunoprecipitation of endogenous JunB from C2C12 myotubes at the sixth day of differentiation were performed using the Direct IP kit (Thermo Fisher Scientific).

ChIP assays and promoter analyses

C2C12 myotubes at the fourth day of differentiation were infected with either mock (GFP), ca-FoxO3, JunB, or JunB with ca-FoxO3 adenoviruses. 2 d after infection, ChIP was performed with ChIP assay kit (Millipore) according to the manufacturer's instructions.

Oligonucleotide primers for amplification of a FoxO binding site on the atrogen-1 promoter are forward -3,228 bp (5'-CTGGCAGGGAGG-AGCCTAATGAATC-3') and reverse -2,966 bp (5'-GGGAGTGGCAAG-CCGTCTC-3'). Oligonucleotide primers for amplification of a JunB site on the atrogen-1 promoter are forward -3,088 bp (5'-TCCCTGCAGGATGA-AATGTT-3') and reverse -2,933 bp (5'-GTATGCCCTGGGTCCAAGT-3'). Oligonucleotide primers for the amplification of a JunB site on the MyHC-2B promoter are forward -1,384 bp (5'-GAGTGGTAGTCAGTCTCTTT-3') and reverse -1,199 bp (5'-TACCCCAAGTGTAGGCTCA-3').

Online supplemental material

Fig. S1 shows images of cryosections of muscles electroporated with JunB shRNA. Fig. S2 shows images of cryosections of muscles treated with BrdU and quantification of myofiber size after cycloheximide treatment. Fig. S3 shows the efficiency of siRNA-mediated knockdown of JunB. Fig. S4 shows the level of overexpression of JunB and ca-FoxO3 in myotubes by transient transfection and by adenoviral infection, the results of the immunoprecipitation of JunB and the interaction with Fos and Fra1. Fig. S5 is a bar diagram showing the mRNA expression mediated by JunB on the mRNAs of atrogen-1, MuRF-1, and on some of the autophagy-related genes. Online supplemental material is available at <http://www.jcb.org/cgi/content/full/jcb.201001136/DC1>.

This work was supported by grants to M. Sandri from Agenzia Spaziale Italiana (Osteoporosis and Muscular Atrophy project), from Telethon-Italy (TCP04009), from the Italian Ministry of Education, University, and Research (PRIN 2007), and from the European Union (MYOAGE; contract 223576 of FP7); to A.L. Goldberg from the National Institute of Aging, the Muscular Dystrophy Association, and a senior fellowship from the Ellison Foundation; and to G. Lanfranchi from the Association Française contre le Myopathies, the Italian Ministry of University and Scientific Research (PRIN 2006), and Veneto Region (Biotech Action). A. Raffaello is a recipient of a postdoctoral fellowship from the University of Padova.

Submitted: 25 January 2010

Accepted: 7 September 2010

References

- Allen, D.L., and T.G. Unterman. 2007. Regulation of myostatin expression and myoblast differentiation by FoxO and SMAD transcription factors. *Am. J. Physiol. Cell Physiol.* 292:C188–C199. doi:10.1152/ajpcell.00542.2005
- Angel, P., M. Imagawa, R. Chiu, B. Stein, R.J. Imbra, H.J. Rahmsdorf, C. Jonat, P. Herrlich, and M. Karin. 1987. Phorbol ester-inducible genes contain a common cis element recognized by a TPA-modulated trans-acting factor. *Cell* 49:729–739. doi:10.1016/0092-8674(87)90611-8
- Angel, P., E.A. Allegretto, S.T. Okino, K. Hattori, W.J. Boyle, T. Hunter, and M. Karin. 1988. Oncogene jun encodes a sequence-specific trans-activator similar to AP-1. *Nature* 332:166–171. doi:10.1038/332166a0
- Bakiri, L., D. Lallemand, E. Bossy-Wetzel, and M. Yaniv. 2000. Cell cycle-dependent variations in c-Jun and JunB phosphorylation: a role in the control of cyclin D1 expression. *EMBO J.* 19:2056–2068. doi:10.1093/emboj/19.9.2056
- Black, F.M., S.E. Packer, T.G. Parker, L.H. Michael, R. Roberts, R.J. Schwartz, and M.D. Schneider. 1991. The vascular smooth muscle alpha-actin gene is reactivated during cardiac hypertrophy provoked by load. *J. Clin. Invest.* 88:1581–1588. doi:10.1172/JCI115470
- Bodine, S.C., E. Latres, S. Baumhueter, V.K. Lai, L. Nunez, B.A. Clarke, W.T. Poueymirou, F.J. Panaro, E. Na, K. Dharmarajan, et al. 2001a. Identification of ubiquitin ligases required for skeletal muscle atrophy. *Science* 294:1704–1708. doi:10.1126/science.1065874
- Bodine, S.C., T.N. Stitt, M. Gonzalez, W.O. Kline, G.L. Stover, R. Bauerlein, E. Zlotchenko, A. Scrimgeour, J.C. Lawrence, D.J. Glass, and G.D. Yancopoulos. 2001b. Akt/mTOR pathway is a crucial regulator of skeletal muscle hypertrophy and can prevent muscle atrophy in vivo. *Nat. Cell Biol.* 3:1014–1019. doi:10.1038/ncb1101-1014
- Brand, T., H.S. Sharma, K.E. Fleischmann, D.J. Duncker, E.O. McFalls, P.D. Verdouw, and W. Schaper. 1992. Proto-oncogene expression in porcine myocardium subjected to ischemia and reperfusion. *Circ. Res.* 71:1351–1360.
- Calnan, D.R., and A. Brunet. 2008. The FoxO code. *Oncogene* 27:2276–2288. doi:10.1038/onc.2008.21
- Chaloux, E., T. López-Rovira, J.L. Rosa, R. Bartrons, and F. Ventura. 1998. JunB is involved in the inhibition of myogenic differentiation by bone morphogenetic protein-2. *J. Biol. Chem.* 273:537–543. doi:10.1074/jbc.273.1.537
- Coletta, D.K., B. Balas, A.O. Chavez, M. Baig, M. Abdul-Ghani, S.R. Kashyap, F. Folli, D. Tripathy, L.J. Mandarino, J.E. Cornell, et al. 2008. Effect of acute physiological hyperinsulinemia on gene expression in human skeletal muscle in vivo. *Am. J. Physiol. Endocrinol. Metab.* 294:E910–E917. doi:10.1152/ajpendo.00607.2007
- Curran, T., and B.R. Franza Jr. 1988. Fos and Jun: the AP-1 connection. *Cell* 55:395–397. doi:10.1016/0092-8674(88)90024-4
- Donà, M., M. Sandri, K. Rossini, I. Dell'Aica, M. Podhorska-Okolow, and U. Carraro. 2003. Functional in vivo gene transfer into the myofibers of adult skeletal muscle. *Biochem. Biophys. Res. Commun.* 312:1132–1138. doi:10.1016/j.bbrc.2003.11.032
- Fan, H.Y., C.G. Cherng, F.Y. Yang, L.Y. Cheng, C.J. Tsai, L.C. Lin, and L. Yu. 2010. Systemic treatment with protein synthesis inhibitors attenuates the expression of cocaine memory. *Behav. Brain Res.* 208:522–527. doi:10.1016/j.bbr.2009.12.034
- Furuno, K., M.N. Goodman, and A.L. Goldberg. 1990. Role of different proteolytic systems in the degradation of muscle proteins during denervation atrophy. *J. Biol. Chem.* 265:8550–8557.
- Glass, D.J. 2005. Skeletal muscle hypertrophy and atrophy signaling pathways. *Int. J. Biochem. Cell Biol.* 37:1974–1984.
- Gomes, M.D., S.H. Lecker, R.T. Jago, A. Navon, and A.L. Goldberg. 2001. Atrogen-1, a muscle-specific F-box protein highly expressed during muscle atrophy. *Proc. Natl. Acad. Sci. USA* 98:14440–14445. doi:10.1073/pnas.251541198
- Gronostajski, R.M., A.L. Goldberg, and A.B. Pardee. 1984. The role of increased proteolysis in the atrophy and arrest of proliferation in serum-deprived fibroblasts. *J. Cell. Physiol.* 121:189–198. doi:10.1002/jcp.1041210124
- Halazonetis, T.D., K. Georgopoulos, M.E. Greenberg, and P. Leder. 1988. c-Jun dimerizes with itself and with c-Fos, forming complexes of different DNA binding affinities. *Cell* 55:917–924. doi:10.1016/0092-8674(88)90147-X
- Hirai, S., and M. Yaniv. 1989. Jun DNA-binding is modulated by mutations between the leucines or by direct interaction of fos with the TGACTCA sequence. *New Biol.* 1:181–191.

- Jagoe, R.T., and A.L. Goldberg. 2001. What do we really know about the ubiquitin-proteasome pathway in muscle atrophy? *Curr. Opin. Clin. Nutr. Metab. Care.* 4:183–190. doi:10.1097/00075197-200105000-00003
- Jagoe, R.T., S.H. Lecker, M. Gomes, and A.L. Goldberg. 2002. Patterns of gene expression in atrophying skeletal muscles: response to food deprivation. *FASEB J.* 16:1697–1712. doi:10.1096/fj.02-0312com
- Kandarian, S.C., and R.W. Jackman. 2006. Intracellular signaling during skeletal muscle atrophy. *Muscle Nerve.* 33:155–165. doi:10.1002/mus.20442
- Lecker, S.H., R.T. Jagoe, A. Gilbert, M. Gomes, V. Baracos, J. Bailey, S.R. Price, W.E. Mitch, and A.L. Goldberg. 2004. Multiple types of skeletal muscle atrophy involve a common program of changes in gene expression. *FASEB J.* 18:39–51. doi:10.1096/fj.03-0610com
- Li, L., J.S. Hu, and E.N. Olson. 1990. Different members of the jun proto-oncogene family exhibit distinct patterns of expression in response to type beta transforming growth factor. *J. Biol. Chem.* 265:1556–1562.
- Mammucari, C., G. Milan, V. Romanello, E. Masiero, R. Rudolf, P. Del Piccolo, S.J. Burden, R. Di Lisi, C. Sandri, J. Zhao, et al. 2007. FoxO3 controls autophagy in skeletal muscle in vivo. *Cell Metab.* 6:458–471. doi:10.1016/j.cmet.2007.11.001
- Markou, T., T.E. Cullingford, A. Giraldo, S.C. Weiss, A. Alsafi, S.J. Fuller, A. Clerk, and P.H. Sugden. 2008. Glycogen synthase kinases 3alpha and 3beta in cardiac myocytes: regulation and consequences of their inhibition. *Cell. Signal.* 20:206–218. doi:10.1016/j.cellsig.2007.10.004
- Medina, R., S.S. Wing, and A.L. Goldberg. 1995. Increase in levels of polyubiquitin and proteasome mRNA in skeletal muscle during starvation and denervation atrophy. *Biochem. J.* 307:631–637.
- Mitch, W.E., and A.L. Goldberg. 1996. Mechanisms of muscle wasting. The role of the ubiquitin-proteasome pathway. *N. Engl. J. Med.* 335:1897–1905. doi:10.1056/NEJM199612193352507
- Mizushima, N., A. Yamamoto, M. Matsui, T. Yoshimori, and Y. Ohsumi. 2004. In vivo analysis of autophagy in response to nutrient starvation using transgenic mice expressing a fluorescent autophagosome marker. *Mol. Biol. Cell.* 15:1101–1111. doi:10.1091/mbc.E03-09-0704
- Passegué, E., and E.F. Wagner. 2000. JunB suppresses cell proliferation by transcriptional activation of p16(INK4a) expression. *EMBO J.* 19:2969–2979. doi:10.1093/emboj/19.12.2969
- Romanello, V., E. Guadagnin, L. Gomes, I. Roder, C. Sandri, Y. Petersen, G. Milan, E. Masiero, P. Del Piccolo, M. Foretz, et al. 2010. Mitochondrial fission and remodelling contributes to muscle atrophy. *EMBO J.* 29:1774–1785. doi:10.1038/emboj.2010.60
- Rommel, C., S.C. Bodine, B.A. Clarke, R. Rossman, L. Nunez, T.N. Stitt, G.D. Yancopoulos, and D.J. Glass. 2001. Mediation of IGF-1-induced skeletal myotube hypertrophy by PI(3)K/Akt/mTOR and PI(3)K/Akt/GSK3 pathways. *Nat. Cell Biol.* 3:1009–1013. doi:10.1038/ncb1101-1009
- Sacheck, J.M., A. Ohtsuka, S.C. McLary, and A.L. Goldberg. 2004. IGF-I stimulates muscle growth by suppressing protein breakdown and expression of atrophy-related ubiquitin ligases, atrogin-1 and MuRF1. *Am. J. Physiol. Endocrinol. Metab.* 287:E591–E601. doi:10.1152/ajpendo.00073.2004
- Sacheck, J.M., J.P.K. Hyatt, A. Raffaello, R.T. Jagoe, R.R. Roy, V.R. Edgerton, S.H. Lecker, and A.L. Goldberg. 2007. Rapid disuse and denervation atrophy involve similar transcriptional changes as muscle wasting during systemic diseases. *FASEB J.* 21:140–155. doi:10.1096/fj.06-6604com
- Sandri, M., C. Sandri, A. Gilbert, C. Skurk, E. Calabria, A. Picard, K. Walsh, S. Schiaffino, S.H. Lecker, and A.L. Goldberg. 2004. Foxo transcription factors induce the atrophy-related ubiquitin ligase atrogin-1 and cause skeletal muscle atrophy. *Cell.* 117:399–412. doi:10.1016/S0092-8674(04)00400-3
- Sandri, M., J. Lin, C. Handschin, W. Yang, Z.P. Arany, S.H. Lecker, A.L. Goldberg, and B.M. Spiegelman. 2006. PGC-1alpha protects skeletal muscle from atrophy by suppressing FoxO3 action and atrophy-specific gene transcription. *Proc. Natl. Acad. Sci. USA.* 103:16260–16265. doi:10.1073/pnas.0607795103
- Sartori, R., G. Milan, M. Patron, C. Mammucari, B. Blaauw, R. Abraham, and M. Sandri. 2009. Smad2 and 3 transcription factors control muscle mass in adulthood. *Am. J. Physiol. Cell Physiol.* 296:C1248–C1257. doi:10.1152/ajpcell.00104.2009
- Serrano, A.L., M. Murgia, G. Pallafacchina, E. Calabria, P. Coniglio, T. Lømo, and S. Schiaffino. 2001. Calcineurin controls nerve activity-dependent specification of slow skeletal muscle fibers but not muscle growth. *Proc. Natl. Acad. Sci. USA.* 98:13108–13113. doi:10.1073/pnas.231148598
- Skurk, C., H. Maatz, H.S. Kim, J. Yang, M.R. Abid, W.C. Aird, and K. Walsh. 2004. The Akt-regulated forkhead transcription factor FOXO3a controls endothelial cell viability through modulation of the caspase-8 inhibitor FLIP. *J. Biol. Chem.* 279:1513–1525. doi:10.1074/jbc.M304736200
- Sng, J.C., H. Taniura, and Y. Yoneda. 2004. A tale of early response genes. *Biol. Pharm. Bull.* 27:606–612. doi:10.1248/bpb.27.606
- Stitt, T.N., D. Drujan, B.A. Clarke, F. Panaro, Y. Timofeyeva, W.O. Kline, M. Gonzalez, G.D. Yancopoulos, and D.J. Glass. 2004. The IGF-1/PI3K/Akt pathway prevents expression of muscle atrophy-induced ubiquitin ligases by inhibiting FOXO transcription factors. *Mol. Cell.* 14:395–403. doi:10.1016/S1097-2765(04)00211-4
- Trendelenburg, A.U., A. Meyer, D. Rohner, J. Boyle, S. Hatakeyama, and D.J. Glass. 2009. Myostatin reduces Akt/TORC1/p70S6K signaling, inhibiting myoblast differentiation and myotube size. *Am. J. Physiol. Cell Physiol.* 296:C1258–C1270. doi:10.1152/ajpcell.00105.2009
- Trenerry, M.K., K.A. Carey, A.C. Ward, and D. Cameron-Smith. 2007. STAT3 signaling is activated in human skeletal muscle following acute resistance exercise. *J. Appl. Physiol.* 102:1483–1489. doi:10.1152/japphysiol.01147.2006
- van der Vos, K.E., and P.J. Coffey. 2008. FOXO-binding partners: it takes two to tango. *Oncogene.* 27:2289–2299. doi:10.1038/onc.2008.22
- Wagner, E.F. 2001. AP-1—Introductory remarks. *Oncogene.* 20:2334–2335. doi:10.1038/sj.onc.1204416
- White, M.E., C.E. Allen, and W.R. Dayton. 1988. Effect of sera from fed and fasted pigs on proliferation and protein turnover in cultured myogenic cells. *J. Anim. Sci.* 66:34–40.
- Wing, S.S., A.L. Haas, and A.L. Goldberg. 1995. Increase in ubiquitin-protein conjugates concomitant with the increase in proteolysis in rat skeletal muscle during starvation and atrophy denervation. *Biochem. J.* 307:639–645.
- Xia, Y., L.M. Buja, R.C. Scarpulla, and J.B. McMillin. 1997. Electrical stimulation of neonatal cardiomyocytes results in the sequential activation of nuclear genes governing mitochondrial proliferation and differentiation. *Proc. Natl. Acad. Sci. USA.* 94:11399–11404. doi:10.1073/pnas.94.21.11399
- Zhao, J., J.J. Brault, A. Schild, P. Cao, M. Sandri, S. Schiaffino, S.H. Lecker, and A.L. Goldberg. 2007. FoxO3 coordinately activates protein degradation by the autophagic/lysosomal and proteasomal pathways in atrophying muscle cells. *Cell Metab.* 6:472–483. doi:10.1016/j.cmet.2007.11.004